Texture and phase analysis of a $Ca_3Co_4O_9$/Si (100) thermoelectric film

W. Wong-Ng,[a] M. D. Vaudin, M. Otani, and N. D. Lowhorn
Ceramics Division, National Institute of Standards and Technology, Gaithersburg, Maryland 20899

Y. F. Hu and Q. Li
Materials Science Department, Brookhaven National Laboratory, Upton, New York 11973

B. He
Bruker AXS, Inc., Madison, Wisconsin 53711

(Received 2 April 2007; accepted 19 June 2007; published online 15 August 2007)

This paper reports the texture analysis as well as the identification of two crystalline phases between a thin film of monoclinic $Ca_3Co_4O_9$ and a cubic (100) Si substrate, using a diffractometer equipped with a two-dimensional area detector. No reflections other than 00ℓ were observed in the symmetric configuration using an x-ray powder diffraction scan (Bragg-Brentano geometry). Pole figures collected for six reflections using asymmetric configurations did not show *ab*-plane epitaxial relationships between the film and the substrate. These results establish the $Ca_3Co_4O_9$ fiber texture of the film with the (001) pole parallel to the surface normal. Single-crystal-like second phases, $CaCoSi_2O_6$ and CoO, presumably the interface reaction products of $Ca_3Co_4O_9$ with the substrate Si, were identified. The near four-fold symmetry and the similar intensity displayed by the 220 reflection from the $CaCoSi_2O_6$ structure indicated an epitaxial relation between $CaCoSi_2O_6$ and Si, with four symmetry-induced variants being generated with approximately equal volume fractions.
© *2007 American Institute of Physics*. [DOI: 10.1063/1.2767613]

I. INTRODUCTION

In response to soaring energy demand, increasing global attention in research and development of thermoelectric materials has developed in recent years. Although thermoelectric materials were discovered more than 170 years ago by Seebeck[1] and Peltier[2] who investigated the now well-known phenomenon of direct conversion between heat and electricity, only a small number of materials have been found to have practical industrial applications. For example, Bi_2Te_3 is one of the principal materials that is being used for cooling application and Si/Ge is used for power conversion. However, these materials offer rather low efficiency which limits their widespread application.

The efficiency and performance of thermoelectric energy conversion or cooling are related to the dimensionless figure of merit (*ZT*) of the thermoelectric (TE) materials, given by

$$ZT = \frac{S^2 \sigma T}{k}, \tag{1}$$

where T is the absolute temperature, S is the Seebeck coefficient or thermoelectric power, σ is the electrical conductivity, and k is the thermal conductivity. *ZT* is directly related to the coefficient of performance of a thermoelectric material and is the reference by which these materials are judged. Thermoelectric materials with desirable properties [high *ZT* ($\gg 1$), i.e., characterized by high electrical conductivity, high Seebeck coefficient, and low thermal conductivity] will have widespread military and industrial applications. In recent years there has been a revival of interest in this field, partly based on reports that relatively high *ZT* values are possible in both thin films and bulk materials.[3,4] For example, Venkatasubramanian *et al.* found *ZT* of about 2.4 at 300 K in Bi_2Te_3/Sb_2Te_3 *p*-type superlattices and 1.4 in $Bi_2Te_3/Bi_2Te_{2.83}Se_{0.17}$ *n*-type superlattices.[5] Other important materials include quantum well films[6] and quantum dot films[7] that yield *ZT* as high as 3.0. In order for the current thermoelectric technology to hold promise for large-scale applications, continued efforts to identify improved materials and optimize existing materials are crucial. Materials that are stable at high temperature would be important for applications in automobile industry.

The discovery of improved thermoelectric oxides has been of great interest to the thermoelectric community, particularly to those who are interested in high-temperature applications, because of the stability of oxides at high temperature. One specific family, the layered cobaltite that includes $NaCoO_x$,[8] $Ca_2Co_3O_6$,[9,10] and $Ca_3Co_4O_9$[11–13] has attracted considerable attention because of the coexistence of large Seebeck coefficient and low resistivity. These compounds also have the characteristic of high electronic anisotropy. Among these members, the $Ca_3Co_4O_9$ phase has the best properties due to its distinctive misfit-layered oxide structure that features two penetrating incommensurate sublattices having the common a, c, and β parameters, but with different b [$a=4.8376(7)$ Å, $b_1=4.5565(6)$ Å, $c=10.833(1)$ Å, and $\beta=98.06(1)°$; $a=4.8376(7)$ Å, $b_2=2.8189(4)$ Å, $c=10.833(1)$ Å, and $\beta=98.06(1)°$, respectively].[12] Along the c axis, triple rocksalt-type Ca_2CoO_3 layers are stacked with single CdI_2-type CoO_2 layers. The interface between these two misfit motifs provides an additional source for phonon scattering, therefore reducing the thermal conductivity. However, although extensive studies have been carried out on these materials in their bulk form, a lesser amount of re-

[a]Electronic mail: winnie.wong-rg@nist.gov

 © 2007 American Institute of Physics

Downloaded 29 May 2008 to 129.6.180.72. Redistribution subject to AIP license or copyright; see http://jap.aip.org/jap/copyright.jsp

search has been performed using thin films. A recent $Ca_3Co_4O_9/Si$ film from Brookhaven National Laboratory showed excellent temperature dependence of resistivity ρ and Seebeck coefficient.[14] One-dimensional (1D) conventional x-ray diffraction showed (001) texture of the film; however, no information pertaining to *ab*-plane texture was obtained.

Crystallographic texture, or preferred crystalline orientation, is an important feature of materials that frequently correlates directly with various physical properties, particularly properties that are strongly anisotropic in nature. Texture analysis is the key to understanding general material properties such as mechanical strength, elasticity, electrical resistance, thermal conductivity, and magnetic and optical properties. Texture analysis using a two-dimensional (2D) area detector is a more efficient process than using a 1D linear diffractometer. This technique allows the direct measurement of the distribution of $(kk\ell)$ poles by studying a fixed and relatively large ($\approx 35°$) 2θ range while varying the sample orientation in the diffractometer. The intensity distribution could be visualized as "intensity mountains" on the pole sphere.

The main goal of this study is to investigate the texture properties of a typical $Ca_3Co_4O_9/Si$ film using a 2D area detector technique. More specifically, it is important to determine if in-plane texture exists in the *ab* plane (approximately normal to the *c* axis of the film) for correlation with the thermoelectric properties of the film. Our second goal is to investigate whether the $Ca_3Co_4O_9/Si$ film contains impurity phases.

II. EXPERIMENT

A. Film preparation

The $Ca_3Co_4O_9$ film was deposited on a commercial Si (100) single crystal wafer in an *in situ* manner using the pulsed laser deposition (PLD) facility. The $Ca_3Co_4O_9$ target was prepared from a stoichiometric mixture of high-purity $CaCO_3$ and Co_3O_4 powders. The powders were homogenized and heat treated twice at 880–890 °C for 24 h in flowing air with intermediate grindings. After pressing the powder into a disk, the final sintering was accomplished at 900 °C for 24 h in flowing O_2 gas. The substrates were cleaned in acetone and methanol prior to deposition, but the native oxide layer on the Si substrate surface was not removed chemically. In general, films about 2300 Å thick were deposited at a substrate temperature of 700 °C with a laser energy density of $\approx 1.5\ J/cm^2$, under an oxygen partial pressure of 39.5 Pa (or 300 mTorr). After deposition, films were cooled to room temperature in ≈0.1 MPa of oxygen.

B. X-ray diffraction of films: Pole figures and phase identification

Data collection for film texture was performed on a Bruker D8 diffractometer[15] with the general area detector diffraction system (GADDS) and a rotating anode, operating at 40 kV and 20 mA. The core of the GADDS is the two-dimensional area detector that is a photon counter over a large area.[16] The goniometer system is oriented horizontally with the sample mounted on a χ, ϕ eucentric cradle so that the film is normal to the (azimuthal) ϕ axis. The cradle rotates about a vertical axis (denoted ω) which changes the orientation of the χ axis in the horizontal plane. The χ rotation controls the orientation of the ϕ axis, and the convention is that χ is 90° when the ϕ axis is horizontal. The 2θ axis is collinear with the ω axis and controls the position of the area detector. Using this diffractometer system the diffraction is not limited to the diffractometer plane. Phase identification can be accomplished by integration along the Debye rings over a selected range of 2θ and χ. One can also obtain both qualitative and quantitative texture information by evaluating the Debye rings. For example, if the Debye rings are continuous and smooth, the sample is polycrystalline and fine grained. If the rings are continuous but spotty, the material is polycrystalline and contains large grains. Incomplete Debye rings indicate orientation or texture. If only individual spots are observed, the material is a single crystal or the extreme case of crystallographic texture. Quantitative evaluation of the Debye rings is discussed in Sec. III A.

In the present study, pole figure constructions were performed using the software system that is part of GADDS.[16] GADDS was used to measure pole figures at fine steps of 2° in ϕ that allow for detection of sharp texture. Data collection for texture analysis has been performed on the Si substrate (using the 111 and 220 reflections), on the $Ca_3Co_4O_9$ film [using the 004 and 005 reflections for determining the (001) texture, and using the 20–1, 11–2, 111, 203, 202, and 020 reflections for in-plane texture study], and on selected phases present in the film/substrate interface. The 2D patterns were recorded with χ values from 10° to 80° and 2θ from 25° to 50°. In this way, one can identify typical reflections from textured phases at χ angles different from 90°. Once the pole figure frames have been collected, Lorentz and polarization correction[17] and integration of the reflection of interest in each of the frames were carried out. At each of the χ angles 10°, 35°, and 60°, 180 frames were collected; and at $\chi = 80°$, 120 frames were collected. The powder x-ray diffraction pattern of the bulk $Ca_3Co_4O_9$ phase that was reported by Masset *et al.*[12] was employed as the reference for the analysis of the present $Ca_3Co_4O_9$ film. During the process of analyzing the two-dimensional x-ray diffraction patterns, we observed a number of small single-crystal-like unknown diffraction peaks. Subsequently, frames of diffraction pattern at different χ and ϕ angles have been studied in further details for phase identification.

III. RESULTS AND DISCUSSION

From the analyses of the x-ray diffraction patterns of the $Ca_3Co_4O_9/Si$ film, we identified the presence of four phases, namely, $Ca_3Co_4O_9$, Si, $CaCoSi_2O_6$, and CoO. The latter two phases were impurity phases detected only when the sample orientation was set with the four-circle goniometer so that the diffracting planes were not parallel to the sample surface; such sample orientations will be referred to as asymmetric. Note that for the symmetric setting, $\chi = 90°$.

The near single crystal property of the Si substrate was confirmed using the pole figures of the 111 (Fig. 1)

Downloaded 29 May 2008 to 129.6.180.72. Redistribution subject to AIP license or copyright; see http://jap.aip.org/jap/copyright.jsp

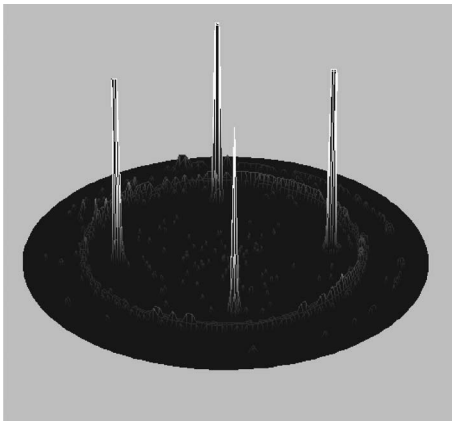

FIG. 1. (111) pole figure of the Si substrate collected over a 2θ range from 28.1° to 28.9°.

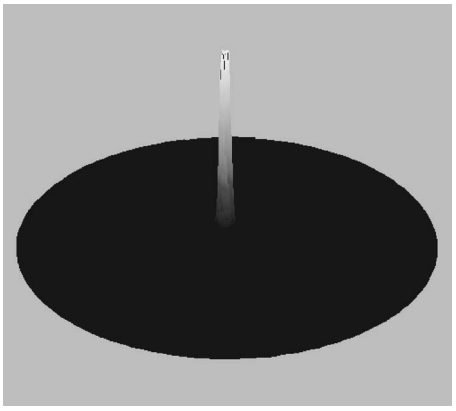

FIG. 3. (005) pole figure of the $Ca_3Co_4O_9$ film deposited on a single crystal Si substrate (2θ range from 41.8° to 42.4°).

reflection.[18] Four sharp and discrete spots are seen in each of these pole figures. Since the Si substrate was fabricated so that the [100] direction is perpendicular to the surface of the substrate, the 111 reflection could only be detected when the χ angle was off 90°.

The following discussion is divided into sections pertaining to the texture study of the $Ca_3Co_4O_9$ film as well as the phase identification of $CaCoSi_2O_6$ and CoO.

A. Texture of the $Ca_3Co_4O_9$/Si (100) film

Figure 2 shows the conventional x-ray diffraction pattern for the $Ca_3Co_4O_9$/Si (100) film. The small peaks indicated by arrows are identified as due to the substrate holder. The only visible peaks in this conventional x-ray pattern are the 00ℓ peaks that indicate (nearly) perfect (001) alignment for the film on the Si substrate. The pole figure of the 005 reflection measured using the area detector (Fig. 3) shows an intense peak at the center, where the χ angle is 90° and the ϕ angle is independent (from 0° to 360°).

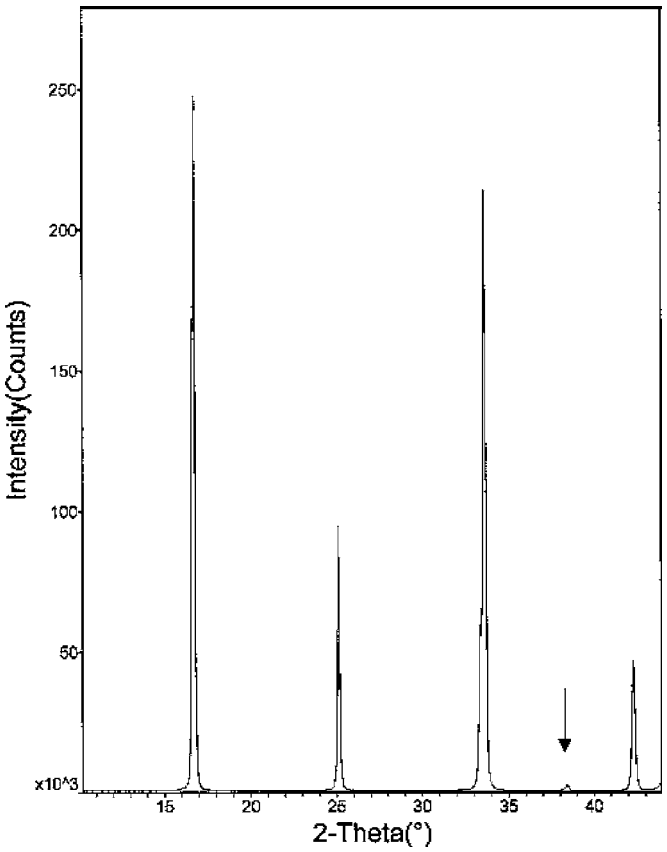

FIG. 2. Powder x-ray diffraction pattern for a $Ca_3Co_4O_9$ film grown on a Si (100) substrate. The small peak in the region between 2θ of 38° and 39° was due to the sample holder.

The (001) texture of the $Ca_3Co_4O_9$ thin film was characterized using an area detector frame in which the 004 and 005 arcs were clearly visible. Integration of the 005 arc gave a texture profile that was perfectly symmetrical about its maximum angle. The two parts of the texture profile on either side of the maximum angle ($\chi<90°$ and $\chi>90°$) were averaged; and the resulting intensity plot $I(\chi)$ is shown in Fig. 4. The volume fraction $V(\alpha)$ of the film with its (001) pole within angle α of the film normal is given by

$$V(\alpha) = \int_0^{\alpha} I(\chi)\sin\chi d\chi \Big/ \int_0^{90} I(\chi)\sin\chi d\chi, \qquad (2)$$

where it is assumed that the intensity is zero from 12° to 90°. Table I shows the results from Eq. (2), which indicate that two-thirds of the film is oriented with (001) within 3° of the

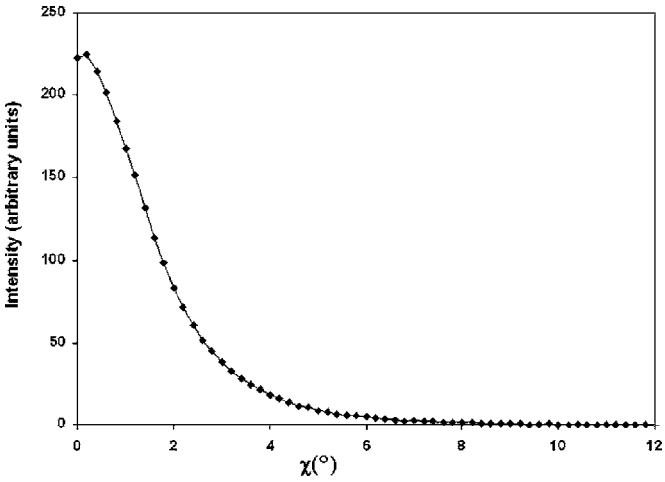

FIG. 4. Averaged texture profile $I(\chi)$ of the 005 reflection.

Downloaded 29 May 2008 to 129.6.180.72. Redistribution subject to AIP license or copyright; see http://jap.aip.org/jap/copyright.jsp

TABLE I. Volume fraction $V(\alpha)$ of the film with its (001) pole within angle α of the film normal.

α°	$V(\alpha)$ (%)
1	18
2	45
3	66
4	80
5	88
6	94
7	97
8	99
9	100

film normal and 94% of the film within 6°. Therefore the sample has an excellent (001) texture.

There is no evidence for any in-plane (*ab* plane) texture for the $Ca_3Co_4O_9$ film. The pole figure obtained using reflection such as 111 (Fig. 5) (which can only be observed with the asymmetric configuration) indicated the absence of an in-plane epitaxial relationship between the film and the substrate. Positions of features on pole figures are characterized by their polar angle α and azimuthal angle β.[16] In these pole figures, strong peaks that represent single-crystal-like texture are absent, while continuous rings of intensity are observed, showing random in-plane orientation of the grains in the film; the ring in Fig. 5 is at $\alpha=68.0°$. These compare very well with the calculated angles in the $Ca_3Co_4O_9$ structure: 67.9° between (001) and (111). It is therefore concluded that the film does not have *ab*-plane texture but has a strong (001) fiber texture. The diffraction spots in Fig. 5 are due to the tail of the strong (111) reflection of the Si substrate.

As discussed in Ref. 14, the thermoelectric properties of the $Ca_3Co_4O_9$ films grown *in situ* by the PLD technique compare well with that of the $Ca_3Co_4O_9$ single crystal.[12] Therefore, the absence of *ab*-plane alignment of the $Ca_3Co_4O_9$ films with the substrate does not appear to be an important factor that contributes to the overall property.

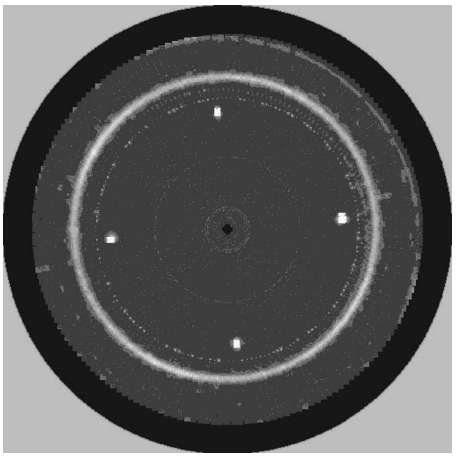

FIG. 5. (111) pole figure (continuous ring) of the $Ca_3Co_4O_9$ film deposited on a single crystal Si substrate (2θ range from 28.4° to 29.4°). The diffraction spots are due to the overlap with the (111) reflection of the Si substrate. A series of rings with very weak intensity are an artifact of data analysis.

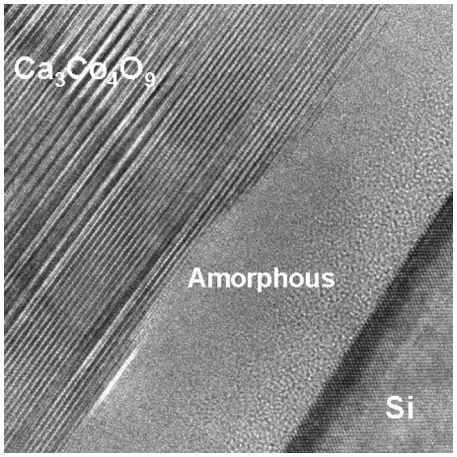

FIG. 6. The high-resolution electron microscopy (HRTEM) image of the $Ca_3Co_4O_9$/Si interface for the film grown on Si (100) substrate, where the *c*-axis-aligned $Ca_3Co_4O_9$ layered structure and single-crystalline Si substrate can be seen. Between the $Ca_3Co_4O_9$ film and Si (100) substrate, there is an amorphous layer with the thickness of ~20 nm.

Strong (001) fiber texture, on the other hand, is critical for achieving good thermoelectric properties.

B. Identification and texture of $CaCoSi_2O_6$ and CoO

Figure 6 shows a high-resolution transmission electron microscopy (HRTEM) image of a typical $Ca_3Co_4O_9$/Si interface region, featuring the atomic $Ca_3Co_4O_9$ layered and single-crystalline Si structure. Between the $Ca_3Co_4O_9$ layer and the Si single crystal, there is typically a 20 nm amorphous layer of material that, in general, exhibits two distinct regions. The region near Si is likely an amorphous SiO_x layer, while the region adjacent to $Ca_3Co_4O_9$ layer is also mainly amorphous, although some unknown crystalline domains were reported previously.[14]

Using the Powder Diffraction File (PDF) (Ref. 19) and Ref. 12, we were able to identify two unknown phases in the $Ca_3Co_4O_9$/Si film from a number of single-crystal-like reflections in the 2D diffraction frames. These phases correspond to $CaCoSi_2O_6$ [monoclinic, $a=9.806(1)$ Å, $b=8.95(1)$ Å, $c=5.243(1)$ Å, and $\beta=105.450(1)°$] (Ref. 20) (Table II) and CoO (hexagonal, $a=3.21$ Å, and $c=5.24$ Å) (Ref. 21) (Table III). Selected 2D detector data for two asymmetric diffractometer settings and the corresponding inte-

TABLE II. Diffractometer settings of 2θ and χ of selected diffraction peaks from the 2D area detector corresponding to the $CaCoSi_2O_6$ phase.

Reflection No.	2θ	χ	h	k	l
1	31.4	18.2	1	3	0
2	29.4	22.5	2	2	1
3	40.9	25.7	0	2	2
			−2	2	2
4	27.4	18.2	2	2	0
5	30.7	25.5	3	1	1
6	38.1	36.2	4	0	0
7	37.4	4.3	1	3	1

Downloaded 29 May 2008 to 129.6.180.72. Redistribution subject to AIP license or copyright; see http://jap.aip.org/jap/copyright.jsp

TABLE III. Diffractometer settings of diffraction peaks from the 2D area detector corresponding to the CoO phase.

Reflection No.	2θ	χ	h	k	l
1	32.4	21.4	1	0	0
2	36.4	23.2	1	0	1

grated powder patterns for the $Ca_3Co_4O_9$/Si film are shown in Figs. 7 and 8. These two figures showed the presence of the $Ca_3Co_4O_9$ and $CaCoSi_2O_6$.

It is likely that the $CaCoSi_2O_6$ and CoO phases are at the interface and their presence is due to the reaction of the $Ca_3Co_4O_9$ film with the Si substrate, or more likely with the SiO_x layer between the film and the substrate according to the following:

$$Ca_3Co_4O_9 + 6SiO_{1.67} \rightarrow 3CaCoSi_2O_6 + CoO. \quad (3)$$

Figure 9 shows the pole figure of the 220 reflection ($2\theta = 27.4°$) of the $CaCoSi_2O_6$ phase. It is noted that the four weak 220 reflections have the same β orientation as the Si 111 reflection, but at a different α angle of 25.5°. The near four-fold symmetry (similar intensity) displayed by the 220 reflection suggests that there is epitaxy between $CaCoSi_2O_6$ and Si, with four symmetry-induced variants being generated in approximately equal volume fractions.

The difficulty of achieving the *ab*-plane epitaxy of the present $Ca_3Co_4O_9$ film may be due to the presence of the amorphous layer of SiO_2 between Si and $Ca_3Co_4O_9$ even before the deposition process (as a result of the reaction of the Si surface with air). This amorphous barrier that is interspersed with small $CaCoSi_2O_6$ and CoO crystallites apparently hampered the function of the single crystal Si to be the template for orienting the film growth in the *ab*-plane direction. The presence of these interfacial phases, however, does not seem to affect the fiber texture.

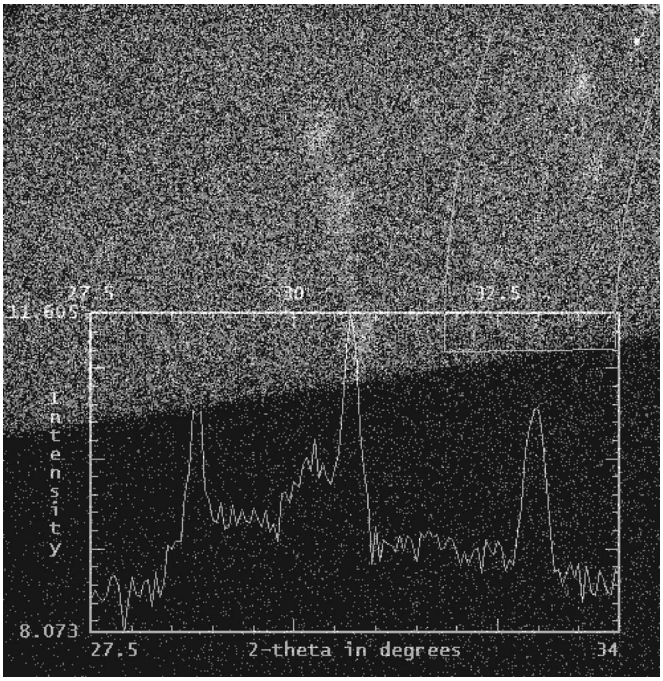

FIG. 8. Two-dimensional detector data and integrated powder pattern for the $Ca_3Co_4O_9$/Si film for 2θ ranging from 27.8° to 34.0°, and with integrated χ from −100° to −114°. The integrated pattern shows the presence of the $Ca_3Co_4O_9$ phase (2θ=28.8° and 33.0°) as well as the $CaCoSi_2O_6$ phase (2θ=30.1° and 30.7°).

IV. SUMMARY

Strong (001) fiber texture of a $Ca_3Co_4O_9$ film on a Si single crystal (100) substrate was established; the 005 pole figure showing a significant degree of texture, while *ab* in-plane texture was absent. The 2D detector allows the successful phase identification of the impurity phases $CaCoSi_2O_6$ and CoO at the $Ca_3Co_4O_9$ and Si interface.

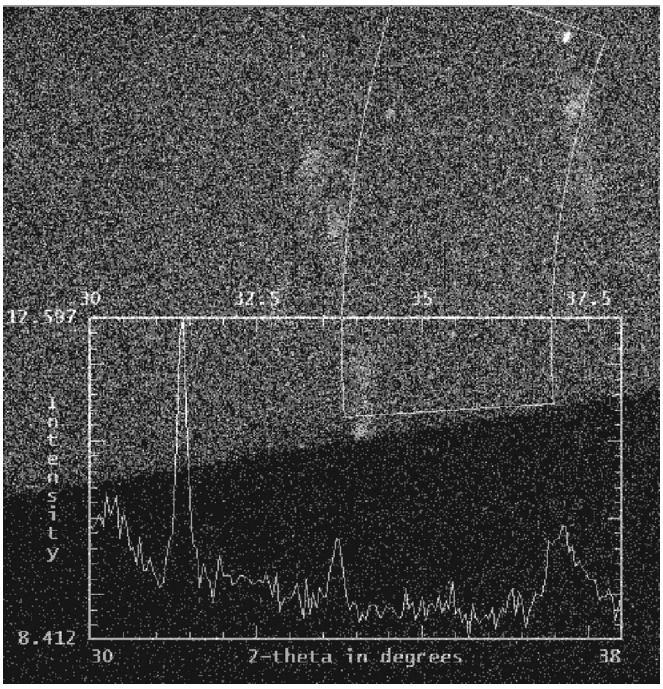

FIG. 7. Two-dimensional detector data and integrated powder pattern for the $Ca_3Co_4O_9$/Si film for 2θ ranging from 30.8° to 37.6°, and with integrated χ from −112.4° to −90.0°. The integrated pattern shows the presence of the $Ca_3Co_4O_9$ phase (2θ=30.3°, 33.5°, and 37.2°) as well as $CaCoSi_2O_6$ (2θ =31.4° and 37.4 °).

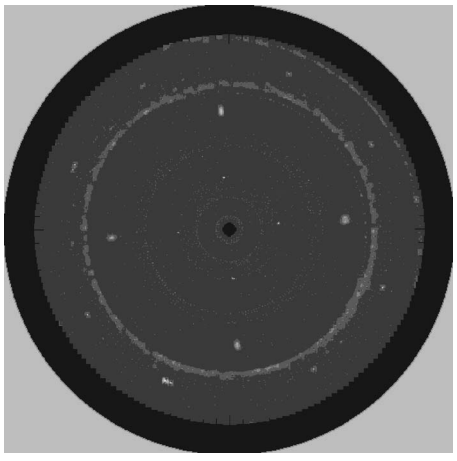

FIG. 9. (220) pole figure (four weak dots near the center) of the $CaCoSi_2O_6$ phase (2θ=27.0°–27.7°). The larger diffraction spots are due to the proximity of the strong (111) reflection of the Si substrate. A series of rings with weak intensity is an artifact of data analysis.

Downloaded 29 May 2008 to 129.6.180.72. Redistribution subject to AIP license or copyright; see http://jap.aip.org/jap/copyright.jsp

These phases are most likely the reaction products of the $Ca_3Co_4O_9$ film with Si according to the reaction: $Ca_3Co_4O_9 + 6SiO_{1.67} \rightarrow 3CaCoSi_2O_6 + CoO$. The presence of the amorphous interface and interfacial crystalline phases appears to have an adverse effect on the epitaxial property of the $Ca_3Co_4O_9$ film on the Si substrate.

[1]T. J. Seebeck, Abhand Deut. Akad. Wiss. Berlin, 265 (1822).
[2]J. C. Peltier, Justus Liebigs Ann. Chem. **LVI**, 371 (1834).
[3]G. S. Nolas, J. Sharp, and H. J. Goldsmid, *Thermoelectric: Basic Principles and New Materials Developments* (Springer, New York, 2001).
[4]T. M. Tritt and M. A. Subramanian, MRS Bull. **31**, p. 188 (2006).
[5]R. Venkatasubramanian, E. Siivola, T. Colpitts, and B. O'Quinn, Nature (London) **413**, 597 (2001).
[6]S. Ghamaty and N. B. Eisner, Proceeding of Interpack 2005: ASME Technical Conference on Packaging of MEMS, NEWS and Electric Systems, 17–22 July 2005, San Francisco, CA (unpublished).
[7]M. S. Dresselhaus, G. Chen, M. Y. Tang, R. G. Yang, H. Lee, D. Z. Wang, Z. F. Ren, J. P. Fleurial, and P. Gogna, Mater. Res. Soc. Symp. Proc., Vol. 886, *Materials and Technologies for Direct Thermal-to-Electric Energy Conversion*, Material Research Society, Boston, MA, Nov. 28-Dec. 2, 2005.
[8]J. Terasaki, Y. Sasago, and K. Uchinokura, Phys. Rev. B **56**, R12685 (1997).
[9]M. Mikami, R. Funashashi, M. Yoshimura, Y. Mori, and T. Sasaki, J. Appl. Phys. **94**, 6579 (2003).
[10]M. Mikami and R. Funahashi, J. Solid State Chem. **178**, 1670 (2005).
[11]D. Grebille, S. Lambert, F. Bouree, and V. Petricek, J. Appl. Crystallogr. **37**, 823 (2004).
[12]A. C. Masset, C. Michel, A. Maignam, M. Hervieu, O. Toulemonde, F. Studer, and B. Raveau, Phys. Rev. B **62**, 166 (2000).
[13]H. Minami, K. Itaka, H. Kawaji, Q. J. Wang, H. Koinuma, and M. Lippmaa, Appl. Surf. Sci. **197**, 442 (2002).
[14]Y. F. Hu, W. D. Si, E. Sutter, and Q. Li, Appl. Phys. Lett. **86**, 082103 (2005).
[15]Certain commercial equipment, instruments, or materials are identified in this paper in order to specify the experimental procedure adequately. Such identification is not intended to imply recommendation or endorsement by the National Institute of Standards and Technology, nor is it intended to imply that the materials or equipment identified are necessarily the best available for the purpose.
[16]Bruker User Manual, General Area Detector Diffraction System (GADDS), vs. 4.9, 1999, Bruker AXS, Inc. Madison, WI 53711.
[17]R. Delhez, E. J. Mittemeijer, Th. H. de Keijser, and H. C. F. Rozendaal, J. Phys. E: J. Sci. Instrum. **10**, 784 (1977).
[18]H. E. Swanson, H. F. McMurdie, M. C. Morris, E. H. Evans, and B. Paretzkin, Natl. Bur. Stand (U.S.) Monogr. **25**, 35 (1976).
[19]Powder Diffraction File (PDF), International Centre for Diffraction Data (ICDD), 12 Campus Blvd., Newtown Square, PA 19081.
[20]S. Ghose, C. Wan, and F. P. Okamura, Am. Mineral. **72**, 375 (1987).
[21]M. J. Redman and E. G. Steward, Nature (London) **193**, 867 (1962).

Downloaded 29 May 2008 to 129.6.180.72. Redistribution subject to AIP license or copyright; see http://jap.aip.org/jap/copyright.jsp